Optical signature of hydrogen-helium demixing at extreme density-temperature conditions

F. Soubiran, S. Mazevet, C. Winisdoerffer, G. Chabrier

Optical signature of hydrogen-helium demixing at extreme density-temperature conditions

F. Soubiran,[1,2] S. Mazevet,[2,3] C. Winisdoerffer,[1] and G. Chabrier[1,4]

[1]*École normale supérieure de Lyon, CRAL, UMR CNRS 5574, Université de Lyon, 69364 Lyon Cedex 07, France*
[2]*CEA DAM-DIF, 91297 Arpajon, France*
[3]*LUTH UMR 8102, Observatoire de Paris, CNRS Université Paris Diderot, 5 place Janssen, 92195 Meudon Cedex, France*
[4]*School of Physics, University of Exeter, Stocker Road, Exeter EX4 4PE, United Kingdom*

By performing direct simulations of demixing for an equimolar mixture of hydrogen and helium, we find that reflectivity measurements performed during dynamic experiments could be used to identify this liquid-liquid phase transition under conditions encountered in giant planet interiors. These first principles simulations show that the reflectivity exhibits a distinctive signature at wavelengths currently available using VISAR (velocity interferometer system for any reflector) measurements. We further make the first estimation of the demixing timescale under such extreme conditions and find that it appears compatible with dynamic measurements.

Hydrogen and helium, as the main baryonic components of the universe, play a key role in determining the mechanical and thermal properties of most astrophysical objects. If the behavior of these materials is well known in the context of high-temperature and low-density plasmas, our knowledge is by far weaker when we enter a low-temperature, high-density regime where N-body effects can no longer be treated as a perturbation. This regime has been loosely named the warm dense matter regime and is common to various domains of astrophysics, high pressure physics, and inertial confinement fusion science. While significant progress has been made to characterize single species plasmas in the past ten years, both on the experimental and theoretical sides, the description of the properties of mixtures and associated phase transitions remains elusive.

The equation of state of the H-He mixture for giant planet and brown dwarf conditions, for instance, remains ill determined. As suggested by Salpeter four decades ago,[1] the H-He mixture can become unstable under giant planet interior conditions and lead to a phase separation. Such a phase separation would drastically affect the structure and the evolution of the planet. This remains so far the most plausible explanation for the excess of Saturn's luminosity at its age.[2,3] In order to test whether such a H/He demixing process occurs under planet interior conditions, several calculations using first principle methods have been performed within the past few years. Morales *et al.*[4] and Lorenzen *et al.*,[5] in particular, performed finite-temperature density functional theory (DFT) molecular dynamics simulations within the generalized gradient approximation (GGA). The first group used thermodynamic integration to estimate the miscibility gap while the second group assumed an ideal entropy of mixing. Both studies find a demixing for helium and hydrogen at temperature and pressure conditions which correspond to a significant fraction of Saturn's interior and to a smaller fraction of Jupiter's interior. Moreover, according to these calculations, demixing occurs at densities and temperatures where hydrogen becomes metallic. As DFT methods are known to underestimate the band gap of semiconductors, the intrication between immiscibility and metallization calls for an experimental validation of these first principle predictions.

Conducting such experiments under conditions relevant to giant planet modeling, however, remains an enormous challenge. This requires first to reach the appropriate conditions and then to identify measurable associated signatures. In the present work, we show that measuring the reflectivity during dynamics experiments using either multishocks or precompressed targets provides a key diagnostic to validate or refute the aforementioned first principle predictions. Indeed, by performing direct simulations of demixing for an equimolar mixture of hydrogen and helium, we first identify a distinctive signature in the reflectivity at wavelengths currently available with VISAR (velocity interferometer system for any reflector) measurements. We further find that the demixing time is compatible with dynamic measurements at these extreme conditions.

These calculations complement previous works recently published by Lorenzen *et al.*[6] and Hamel *et al.*[7] In the first case, the authors identify that demixing occurs naturally in the simulations after about 1 ps. In Hamel *et al.*, they calculate optical properties in the demixing region by assuming that a simulation cell split into two, with hydrogen on one side and helium on the other one, is representative of a demixed state. In contrast, we used here the fact that demixing occurs naturally in the simulation to follow the evolution of the optical properties in time. This allowed us to identify an optical signature for demixing and for a state representative of what occurs on time scales comparable to the ones we have in dynamic experiments.

All the finite-temperature density functional theory molecular dynamics (DFT-MD) simulations were performed using the ABINIT package,[8–10] with 128 nuclei (64 H and 64 He) in a cubic box and periodic boundary conditions. The convergence of the main results presented in this paper was checked using up to 512 atoms in the simulation cell. The choice of an equimolar H/He mixture was dictated by the necessity to minimize finite-size effects when exploring the occurrence or the absence of a phase separation, which is the very aim of the present study. Indeed a 90%/10% mixture would reduce the number of helium particles to 12, making the results of dubious validity. The simulations were performed in the isokinetic ensemble[11,12] where the temperature is kept fixed by a direct rescaling of the velocities. The electronic part was calculated within the generalized gradient approximation (GGA) and using the Perdew, Burke, and Ernzerhof exchange-correlation functional.[13] The temperature dependence was obtained using the Mermin's approach[14]

with a Fermi-Dirac occupation of the electronic band states. We built two sets of projected augmented waves (PAW) pseudopotentials[15,16] in order to prevent any overlap of the PAW spheres for the entire density range presently explored.

For densities smaller than 1.5 g/cm^3, we used pseudopotentials with $r_{cut} = 1.0a_0$ (where a_0 is the Bohr radius). For higher densities, we set $r_{cut} = 0.7a_0$ for hydrogen and $0.6a_0$ for helium which lead to a much larger plane-wave cutoff. All the MD calculations were performed at the Γ point, which provides well converged results for the dynamics: The convergence of our results (better than 2% on the pressure and 0.5% on the internal energy) has been established using simulations with up to a 4^3 Monkhorst-Pack **k**-point grid.[17] We used therefore 192 bands and up to 60 Ha for the cutoff energy of the plane-wave basis. But this had been adapted according to the set of PAW pseudopotentials. The time evolution was done with a time step of 0.48 fs, shorter than the oscillation period of the H$_2$ molecule. For the initial configuration, we placed the hydrogen and helium atoms on a NaCl-like structure. We checked that the initial state chosen did not influence either the demixing time scales or the final states by considering a homogenous liquid state as obtained at higher temperatures as another initial configuration. We also checked the case of a fully unmixed state as an initial condition with no relevant differences.

Finally, the electrical conductivity and the other transport properties such as the reflectivity were obtained using the Kubo-Greenwood formula[18–21] on a set of snapshots extracted from the MD simulations. The optical properties were calculated using up to a 4^3 Monkhorst-Pack **k**-point grid. The convergence of our results was tested by using up to a 8^3 grid. The number of bands was adapted according to the box size and the temperature, in order to get around 1 Ha of unoccupied bands for fully resolved calculations of the properties up to a 1 Ha excitation.

When performing simulations for density-temperature conditions where demixing was previously identified, we observed a clear transition from an initial homogeneous state to a clearly inhomogeneous state during the simulation. Figure 1 shows a representative simulation where we plot the trajectories of every particle over 400 time steps. The difference between the homogeneous case and the demixed one is quite obvious. On the left, the hydrogen atoms are quite scattered and the trajectories are unlocalized, as expected in a homogeneous
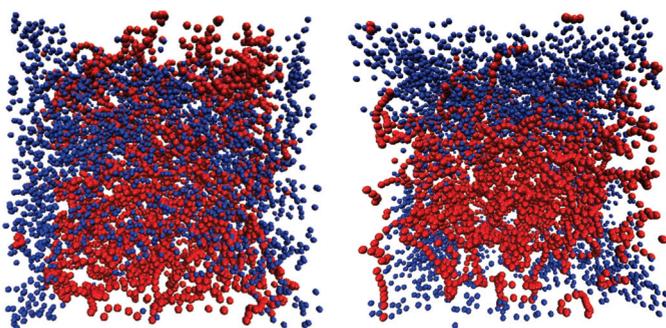
state. On the right, we clearly see two distinct patches as the two species tend to remain separated. The clear occurrence of demixing in direct molecular dynamics simulations was already pointed out in Lorenzen *et al.*[5] We further find in all the performed simulations that the system demixes with a concentration for the dominant species larger than 80% in each identified patch. The concentration in the helium and hydrogen rich regions were obtained by simply counting the number of atoms of each species in the corresponding volume.

While direct inspection of the simulations does not provide a quantitative criteria to establish a phase diagram with precise boundaries for the liquid-liquid phase transition, it still provides a good estimate of the density-temperature conditions at which demixing occurs. Figure 2 summarizes our results and shows the conditions where demixing was identified. We find that, for pressures above one Mbar and temperatures below 12 000 K, the system is always phase separated. We also find a clear temperature dependence, with the system remaining inhomogeneous at higher temperatures as the pressure increases.

We note that we recover the high temperature demixing boundary identified by Lorenzen *et al.* While this is encouraging in a way, this also raises some issues on the ways of studying demixing transition. As molecular dynamics simulations do not provide the ionic entropy, Lorenzen *et al.* added an ideal entropy of mixing to their simulations results neglecting the contributions of the interactions in the entropy. Then they used the Gibbs free energy method to identify the demixing line. But as the simulations directly lead to an inhomogeneous state, we are clearly in a situation where not only the entropy of mixing is questionable, but also the difference in enthalpy as we are considering a demixed state. The Gibbs free energy method, using the relative evolution of this quantity as a function of the concentration of each species, supposes that the system is homogeneous for each concentration which is clearly not the case in our simulations. We are unable to quantify the impact of
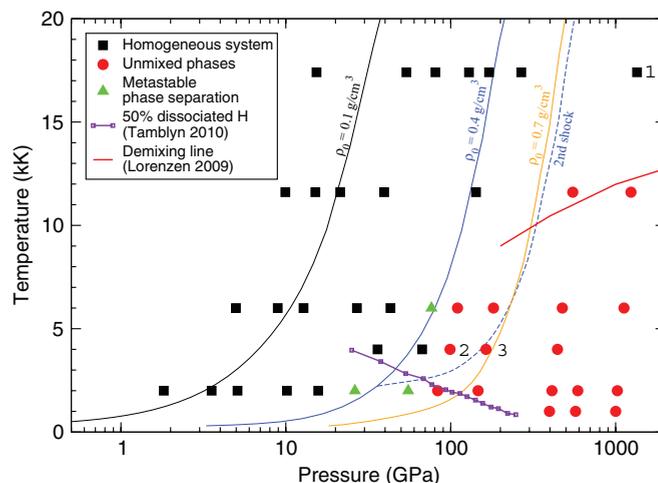

(a) Homogeneous state.   (b) Demixed phases.

FIG. 1. (Color online) Trajectories of hydrogen (blue) and helium (red) nuclei over 400 time steps for an equimolar mixture at 1.50 g/cm^3 and 4000 K at two different stages of the simulation.

FIG. 2. (Color online) Demixing diagram for equimolar mixtures of hydrogen and helium. We plotted the dissociation line for pure hydrogen[22] and the demixing line as previously calculated by Lorenzen *et al.*[5] for an equimolar system. Black, blue, and orange full lines correspond to different Hugoniot curves calculated using the SCvH EOS[23] and with specific precompression densities ρ_0. The dashed line shows a second shock Hugoniot for $\rho_0 = 0.4$ g/cm^3.

these inhomogeneities on the thermodynamic quantities as we were unable to detect a clear difference in the thermodynamic averages between homogeneous and demixed phases. But we would like to stress that, formally, the Gibbs free energy procedure is only valid when considering an homogenous state.

As a close relationship between dissociation and metallization has been previously established for hydrogen,[24–26] a direct comparison with the molecular hydrogen dissociation line established by Tamblyn *et al.*[22] also indicates that demixing occurs in the range of parameters for which hydrogen is metallic. However, the exact relative location of the demixing toward the dissociation/metallization of hydrogen is quite tough to identify as the latter appears to be a continuous phase transition for temperatures higher than 2000 K.[27]

We note that performing microcanonical simulations across the liquid-liquid phase transition may potentially lead to a jump in the temperature at the phase boundary. If it exists, this could be used as a criteria for demixing. As the thermodynamic quantities do not show significant changes across the transition, we believe, however, that it would not reflect in a significant temperature jump. We thus choose to remain in the isokinetics ensemble as it provides a comparison between homogenous and demixed states at the same density and temperature conditions. The small variations of the thermodynamic averages across the liquid-liquid transition also suggest a small influence on the thermostating scheme used on the resulting demixed states.

In Fig. 2, we also indicate the few conditions for which we were not able to clearly identify the state of the system. For these simulations, we observed a transient inhomogeneous state, not always clearly well-defined. This occurs at low temperatures and close to what we have established as the low-temperature, low-pressure boundary for the liquid-liquid phase transition. In this domain, the size of the simulation box is clearly an issue when trying to accurately determine this boundary, as the size of the helium-rich bubbles in the demixed phase at equilibrium is way out of reach of current *ab initio* simulation capabilities. This problem applies to any method aimed at predicting the exact density-temperature location for the phase boundary in the low-temperature regime, either direct simulations like the present ones, or thermodynamic integration as used in previous works.

Using the SCvH EOS,[23] we also display in Fig. 2 the pressure-temperature conditions that can be reached in dynamic experiments using various compression schemes. According to these predictions, the conditions required for demixing can be reached either with precompressed targets (as done for hydrogen and helium[28–30]) or with multiple shock techniques. The required target precompression (around 0.7 g/cm^3) can be achieved using diamond anvil cell (DAC). However, due to technical limitations of current high energy lasers, such a high initial density will be out of reach of single shock experiments to explore the relevant domain of the Hugoniot curve. Fortunately, double shock experiments need a lower initial precompression and can reach the density-temperature conditions required for demixing. The trajectory of such a shock is indicated in Fig. 2. This immediately raises the question of the kinetics of the transition. The kinetics of demixing for a sample initially in a homogeneous state and dynamically brought to these high-pressure conditions is a key issue to experimentally validate the theoretical predictions.

As the simulations were all started from a homogeneous state, we can address this problem and explore the kinetics of the liquid-liquid transition. For the simulations performed in the demixed phase, the careful analysis of the simulation movies showed, for some of them, a transient metastable homogeneous state before the phase transition, which occurs after a substantial delay. Using simulations which show both a metastable homogeneous phase and a stable demixed one, we sought a quantitative criterion that could be used first as a diagnostic to detect the phase transition in an experiment and second to estimate its kinetics.

Following the time evolution of the thermodynamic quantities (pressure, energy) does not provide a valid criterion to differentiate these two situations, as the observed variations are too tiny compared to the standard deviation of these observables. Results for the transport and optical properties, on the other hand, are illustrated in Figs. 3–5. The first simulation (Fig. 3) was performed at $\rho = 3.57$ g/cm^3 and T = 17 406 K and is labeled "1" in Fig. 2. For these conditions, no phase transition occurs. We only observe fluctuations of the reflectivity around the mean value with a standard deviation of about 5%.

In contrast, Figs. 4 and 5 display the results of two simulations for density-temperature conditions for which demixing occurs, at 1.50 g/cm^3 and 4000 K (label "2" in Fig. 2) and 2.39 g/cm^3 and 4000 K (label "3" in Fig. 2), respectively. These two examples show basically the same features. We see a first plateau corresponding to the equilibration of the homogeneous state and then an abrupt evolution of the reflectivity as the system transits to the demixed state. In both cases, the phase transition exhibits a signature on the reflectivity well above statistical fluctuations at the two chosen representative wavelengths. The reflectivity at 1064 nm (resp. at 532 nm) rises from 0.15 to 0.21 (resp. from 0.125 to 0.17) for the run at 1.50 g/cm^3 - 4000 K, and from 0.33 to 0.46 (resp. from 0.256 to 0.34) for the one at 2.39 g/cm^3 - 4000 K. The time corresponding to the rise in the average reflectivity was used to estimate the kinetics of the liquid-liquid phase
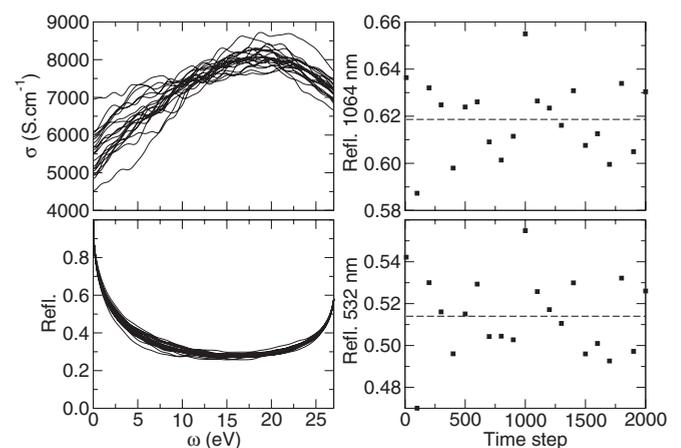

FIG. 3. Results for a simulation at 3.57 g/cm^3 and 17 406 K. On the left hand side is plotted the frequency dependance of the electrical conductivity and the reflectivity at different time steps. On the right hand side is plotted the time evolution of the reflectivity for two specific excitations with the mean value given by the dashed line. We choose 1064 nm and 532 nm excitation wavelengths as they are the most commonly used as probe in laser-driven experiments.
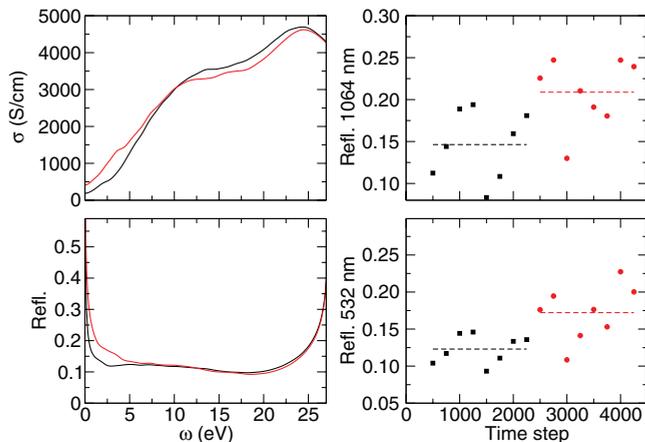
FIG. 4. (Color online) Results for a simulation at 1.50 g/cm³ and 4000 K. On the left hand side is plotted the frequency dependance of the electrical conductivity and the reflectivity in the homogeneous state (black line) and in the demixed one (red dashed line). On the right hand side we plotted the time dependance of the reflectivity at 532 nm and 1064 nm with black square symbols for the homogeneous state and red circle symbols for the demixed one. The dashed lines represent the mean value of the reflectivity for each state.

FIG. 5. (Color online) Results for a simulation at 2.39 g/cm³ and 4000 K. On the left hand side is plotted the frequency dependance of the electrical conductivity and the reflectivity in the homogeneous state (black line) and in the demixed one (red dashed line). On the right hand side we plotted the time dependance of the reflectivity at 532 nm and 1064 nm with black square symbols for the homogeneous state and red circle symbols for the demixed one. The dashed lines represent the mean value of the reflectivity for each state.

transition. For these two density-temperature conditions, we get respectively 0.6 and 1.2 ps. Using rough estimates of the skin depth $\delta = \sqrt{\frac{2}{\omega \mu_0 \sigma}}$ (Ref. 31) probed by the laser probe (where σ is the conductivity, ω the pulsation of the laser, and μ_0 the magnetic constant) and of the shock wave velocity v_s (about 10 km.s⁻¹), we found that the typical time scale of the experiment δ / v_s is much longer than a picosecond, which means that the transition is fast enough to be detected in laser-driven experiments. This conclusion is even reinforced by the fact that the nucleation barrier is more easily overcome in a shock than in a cubic box with periodic boundary conditions.

Furthermore, we see that the homogeneous phase remains stable longer when the reflectivity of the system is lower. The transition occurs twice as slowly for a reflectivity of about 0.15 than for 0.3. This fact that the system remains a shorter time in a homogeneous state as the conductivity/reflectivity increases implies that atomic helium segregates faster as hydrogen becomes more conducting. This correlation between the propensity of hydrogen and helium to demix and the increasing hydrogen conductivity brings support to the suggestion that demixing stems from the difficulty for neutral helium to perdure as a single entity in a metallic fluid of dissociated, ionized hydrogen.

Using reflectivity measurements as a signature for demixing in H-He has already been suggested by Hamel et al.[7] These authors did not identify any clear signature in the reflectivity at photon energies below 3 eV. One important difference with their results, however, is that the present calculations are dealing with situations where the system has reached equilibrium in a demixed state naturally provided by the simulation. Uncertainties remain regarding the influence of the limited number of particles, and, consequently, of the size of the helium-rich droplets. We believe, however, that these states are representative of the non-fully-equilibrated states that could be probed on a ps time scale in dynamic
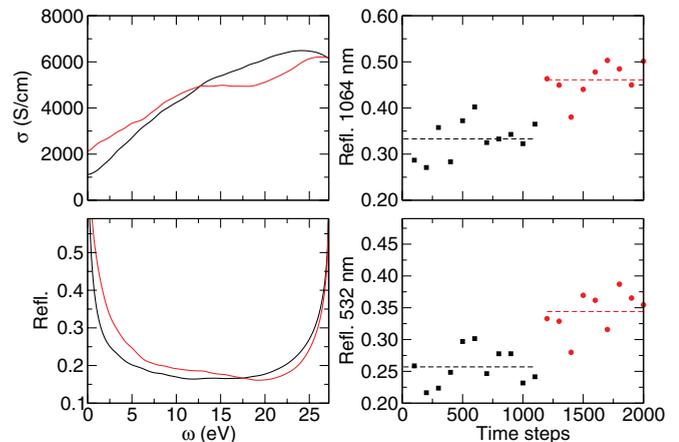
experiments. This contrasts with Hammel et al. who made strong assumptions regarding the nature of these states as they considered (for their conductivities calculations) that hydrogen and helium were completely split apart into two pure phases. Furthermore, previous studies on hydrogen and helium show that ab initio simulations can reproduce rather accurately the variations of reflectivities in extreme conditions. The presently predicted 15% or more differences in reflectivity between the homogeneous and demixed states should be detectable in laser-driven experiments, for which the typical uncertainty for this kind of measurements is about 5–10 %. Reflectivity measurements at standard VISAR wavelengths can thus be used as direct signatures of demixing under extreme conditions when compared to ab initio simulations.

In summary, we show in this article that the demixing of equimolar H-He mixture in the warm dense matter regime, characteristic of many astrophysical body interior conditions, can be probed in laboratory with reflectivity measurements at standard wavelengths. We also provide an estimate for the kinetics of the liquid-liquid phase transition and show that it is compatible with the time scale accessible in current laser experiments. Moreover, even though the required precompression for a single shock experiment precludes any exploration of the relevant density-temperature conditions, this latter can be reached with double shock techniques.

[1] E. E. Salpeter, Astrophys. J. **181**, L83 (1973).

[2] D. J. Stevenson and E. E. Salpeter, Astrophys. J. Suppl. Ser. **35**, 239 (1977).

[3] J. J. Fortney and W. B. Hubbard, Astrophys. J. **608**, 1039 (2004).

[4] M. A. Morales, E. Schwegler, D. Ceperley, C. Pierleoni, S. Hamel, and K. Caspersen, Proc. Natl. Acad. Sci. **106**, 1324 (2009).

[5] W. Lorenzen, B. Holst, and R. Redmer, Phys. Rev. Lett. **102**, 115701 (2009).

[6] W. Lorenzen, B. Holst, and R. Redmer, Phys. Rev. B **84**, 235109 (2011).

[7] S. Hamel, M. A. Morales, and E. Schwegler, Phys. Rev. B **84**, 165110 (2011).

[8] X. Gonze, G. Rignanese, M. Verstraete, J. Beuken, Y. Pouillon, R. Caracas, F. Jollet, M. Torrent, G. Zerah, M. Mikami, P. Ghosez, M. Veithen, J. Raty, V. Olevano, F. Bruneval, L. Reining, R. Godby, G. Onida, D. Hamann, and D. Allan, Z. Kristallogr. **220**, 558 (2005).

[9] X. Gonze, B. Amadon, P. M. Anglade, J. M. Beuken, F. Bottin, P. Boulanger, F. Bruneval, D. Caliste, R. Caracas, M. Cote, T. Deutsch, L. Genovese, P. Ghosez, M. Giantomassi, S. Goedecker, D. R. Hamann, P. Hermet, F. Jollet, G. Jomard, S. Leroux, M. Mancini, S. Mazevet, M. J. T. Oliveira, G. Onida, Y. Pouillon, T. Rangel, G. M. Rignanese, D. Sangalli, R. Shaltaf, M. Torrent, M. J. Verstraete, G. Zerah, and J. W. Zwanziger, Comput. Phys. Commun. **180**, 2582 (2009).

[10] "The ABINIT code is a common project of the Université Catholique de Louvain, Corning Incorporated, and other contributors", http://www.abinit.org.

[11] F. Zhang, J. Chem. Phys. **106**, 6102 (1997).

[12] P. Minary, G. J. Martyna, and M. E. Tuckerman, J. Chem. Phys. **118**, 2527 (2003).

[13] J. P. Perdew, K. Burke, and M. Ernzerhof, Phys. Rev. Lett. **77**, 3865 (1996).

[14] N. D. Mermin, Phys. Rev. **137**, A1441 (1965).

[15] P. E. Blöchl, Phys. Rev. B **50**, 17953 (1994).

[16] N. A. W. Holzwarth, A. R. Tackett, and G. E. Matthews, Comput. Phys. Commun. **135**, 329 (2001).

[17] H. J. Monkhorst and J. D. Pack, Phys. Rev. B **13**, 5188 (1976).

[18] W. A. Harrison, *Solid State Theory* (McGraw-Hill, New York, 1970).

[19] G. D. Mahan, *Many Particle Physics* (Plenum Press, New York, 1981).

[20] J. Callaway, *Quantum Theory of the Solid State* (Academic Press, New York, 1974).

[21] S. Mazevet, M. Torrent, V. Recoules, and F. Jollet, HEDP **6**, 84 (2010).

[22] I. Tamblyn and S. A. Bonev, Phys. Rev. Lett. **104**, 065702 (2010).

[23] D. Saumon, G. Chabrier, and H. Vanhorn, Astrophys. J. Suppl. Ser. **99**, 713 (1995).

[24] L. A. Collins, S. R. Bickham, J. D. Kress, S. Mazevet, T. J. Lenosky, N. J. Troullier, and W. Windl, Phys. Rev. B **63**, 184110 (2001).

[25] M. A. Morales, C. Pierleoni, E. Schwegler, and D. M. Ceperley, Proc. Natl. Acad. Sci. **107**, 12799 (2010).

[26] W. Lorenzen, B. Holst, and R. Redmer, Phys. Rev. B **82**, 195107 (2010).

[27] B. Holst, M. French, and R. Redmer, Phys. Rev. B **83**, 235120 (2011).

[28] P. Loubeyre, P. Celliers, D. Hicks, E. Henry, A. Dewaele, J. Pasley, J. Eggert, M. Koenig, F. Occelli, K. Lee, R. Jeanloz, D. Neely, A. Benuzzi-Mounaix, D. Bradley, M. Bastea, S. Moon, and G. Collins, High Press. Res. **24**, 25 (2004).

[29] J. Eggert, S. Brygoo, P. Loubeyre, R. S. McWilliams, P. M. Celliers, D. G. Hicks, T. R. Boehly, R. Jeanloz, and G. W. Collins, Phys. Rev. Lett. **100**, 124503 (2008).

[30] P. M. Celliers, P. Loubeyre, J. H. Eggert, S. Brygoo, R. S. McWilliams, D. G. Hicks, T. R. Boehly, R. Jeanloz, and G. W. Collins, Phys. Rev. Lett. **104**, 184503 (2010).

[31] J. D. Jackson, *Classical Electrodynamics* (Wiley, New York, 1999).